Available online at www.sciencedirect.com
ScienceDirect
Radiation Physics and Chemistry 75 (2006) 1744–1748
Radiation Physics and Chemistry
www.elsevier.com/locate/radphyschem

A status report on experimental tests of QED in medium-Z systems

Mark N. Kinnane, J.A. Kimpton, C.T. Chantler*

School of Physics, University of Melbourne, Vic. 3010, Australia

Accepted 21 September 2005

Abstract

The electron beam ion trap has opened the door for experimental physics to perform critical tests of bound state QED in the medium-Z regime. The relatively small uncertainties associated with the theoretical predictions necessitate highly accurate experimental measurements of atomic transition energies. This work presents an overview of the issues and key concepts involved in the field. It also demonstrates several major steps taken to suppress systematic uncertainties that have limited past work and presents an error budget for current and future work.

PACS: 32.30.Rj; 07.85.Fv; 07.85.Nc; 39.30.+w; 07.77.Ka

Keywords: X-ray spectra; He-like ions; Electron beam ion traps; Quantum electrodynamics; X-ray detectors

1. Introduction

Second quantisation, the quantisation of the radiation field, was one of the key developments in modern physics during the 20th century. The subject of quantum field theory quickly followed, the application of which to systems of charged particles led to the formulation of the theory of quantum electrodynamics (QED). This fully quantised theory describes the force in terms of particle exchange and, in the case of electromagnetic fields, these particles are virtual photons.

The application of QED to the calculation of energy levels of charged particles in bound systems is usually presented in terms of "bound state" QED. One of the first successful applications of bound state QED was the explanation of the Lamb Shift, the separation of the $2s_{1/2}$ and $2p_{1/2}$ level energies in neutral hydrogen as compared to the degenerate energies predicted by the relativistic Dirac equation.

A problem with free particle QED lies in the difficulty in obtaining exact solutions to the calculations involved and thus in obtaining predictions for measurable quantities such as energy (Karshenboim, 2004; Eides et al., 2001). Calculations such as those involved in scattering or decay problems present a particular challenge due to the number and complexity of the interactions (virtual particle exchanges) between the field and the bodies of interest that must be considered. Bound state QED calculations on the other hand generally consider a more efficient parametrisation. However, the presence of the nucleus and the corresponding static nuclear field requires the consideration of many body and strong coulombic effects. Divergent integrals commonly appear in the calculations requiring regularisation and renormalisations of mass and charge. Further, the selection of a finite number of terms from

*Corresponding author.
E-mail address: chantler@physics.unimelb.edu.au (C.T. Chantler).

0969-806X/$ - see front matter © 2006 Elsevier Ltd. All rights reserved.
doi:10.1016/j.radphyschem.2005.09.017

the infinite perturbative expansions involved, affects the final result. To date high-accuracy results have only been achieved for one or two electron systems due to the difficulty associated with many-body effects.

Developments in computational speed and in mathematical techniques have progressed to the point that calculations now result in predictions for measurable quantities with quoted accuracies on the parts per million level or less. However, the problems mentioned above and how they are treated yield results for different methods often varying by amounts significantly larger than the quoted uncertainties.

Recent developments in experimental techniques make first order bound state QED theory one of the best tested theories of modern physics (Niering et al., 2000). However, these tests primarily probe the lowest order bound state QED contributions. Testing higher order bound state QED calculations and correlated QED can challenge and drive the development of theory.

QED contributions are experimentally tested by measuring the Lamb Shift. The effect was first observed by Lamb and Retherford in experiments performed on the hydrogen atom and has been defined as the difference between the electron energy level predicted by the Dirac theory and that which is observed experimentally (Drake, 1988). The shift is dominated by finite nuclear size contributions (the Dirac theory treats the nuclear potential as a point source) and bound state QED effects. If we accept that, to first order, effects other than the higher order bound state QED contributions are known to a sufficiently high level of accuracy, then any high-accuracy measurement of the X-ray transition energies can probe the higher order predictions (Fig. 1).

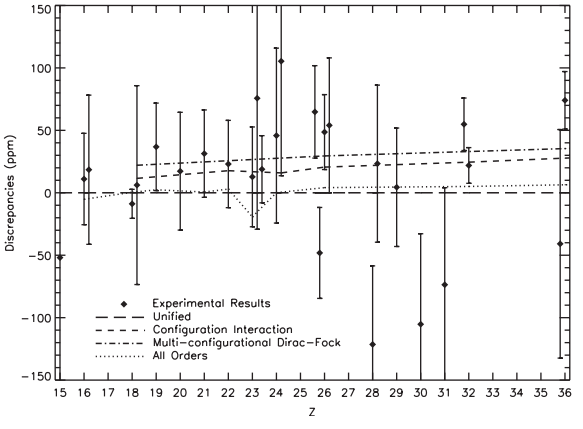

Fig. 1. Theoretical discrepancies relative to Drake (1988) in the medium-Z regime for transition energies in helium-like systems (Chen et al., 1993; Indelicato, 1988; Plante et al., 1994). The experimental uncertainties cover the variation between calculations.

2. Experimental conditions and source

Investigation of bound state QED and the Lamb Shift require few electron atomic systems. Theory is best formulated for one and two electron systems. However, the differences between theoretical calculations for $2p_x$–$1s_x$ transition energies of highly charged ions (HCI) in the medium-Z regime are of order 30 ppm of the total transition energy. Therefore, experimental tests require uncertainties less than this for a critical comment on the computations.

Thermal effects on the resulting X-ray spectral lines contribute to broadenings on the observed peaks that can cause problems especially when observing transitions nearby. The observed ions must be relatively cold.

Medium-Z ions are ideal as the higher order QED contributions scale as $(Z\alpha)^4$. The higher the atomic number, the lower the precision of measurement required to critically measure the higher orders or correction. However, if the ion used has a very large Z then non-QED effects such as those due to the finite nuclear size dominate the shift, making it difficult to extract the bound state QED contribution.

Fast-beam experiments, involving the creation of HCI via beam-foil stripping, and plasma techniques, such as those performed at Tokamak sources, have been limited by bulk motion Doppler shifts and spectral contamination due to the number of competing ion species, making calibration of the system difficult. Uncertainties of order 100–1000 ppm in results from these techniques are not uncommon. Promising techniques include laser resonance spectroscopy (Myers et al., 1996; Silver et al., 1994) and recoil ion spectroscopy to observe transition energies in highly charged argon (Deslattes et al., 1984). However, further work is required in these areas.

The work presented here makes use of an electron beam ion trap (EBIT) for the production of highly charged titanium ions (Ti^{20+}). This device allows the creation, trapping and cooling of highly charged medium to high Z ions and has made significant improvements in the experimental testing of bound state QED. The advantages of the EBIT over other sources are the suppression of the Doppler shift (there is no bulk motion of the ions), a suppression of Doppler broadening (the ions are cooled and confined spatially to a small region), and low satellite contamination (charge state selection is well determined by the kinetic energy of the electron beam used to create the trap potentials).

Fig. 2 shows one of the Ti^{20+} spectra recorded at the NIST EBIT. The relative intensities in this raw data are affected by the (known) response function of the detector system. The w, x, y and z transition lines are clearly visible as well as two lithium-like titanium transition lines, indicating some minor and well separated contamination of the trap with other ionic species.

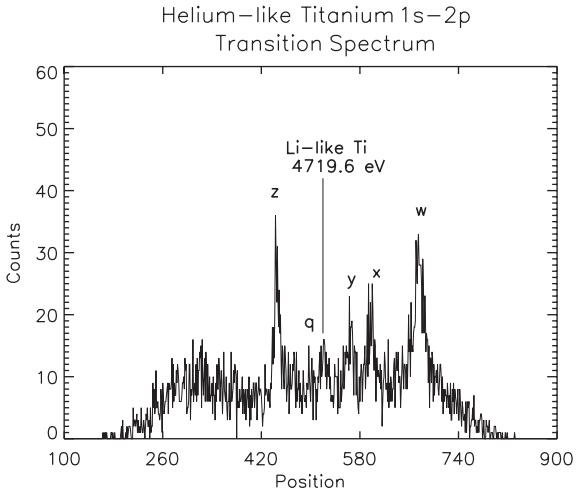

Fig. 2. Single spectrum of Ti^{20+} resonances recorded at the NIST EBIT. The so-called *w*, *x*, *y* and *z* transition lines are clearly visible as well as two lithium-like titanium transition lines, indicating the presence of a small amount of lithium-like ions in addition to the helium-like ions: *w*: He-like Ti($^1S_0-^1P_1$), *x*: He-like Ti($^1S_0-^3P_2$), *y*: He-like Ti($^1S_0-^3P_1$), *q*: Li-like Ti($^2P^0_{1/2}-^2D_{3/2}$), *z*: He-like Ti($^1S_0-^3S_1$).

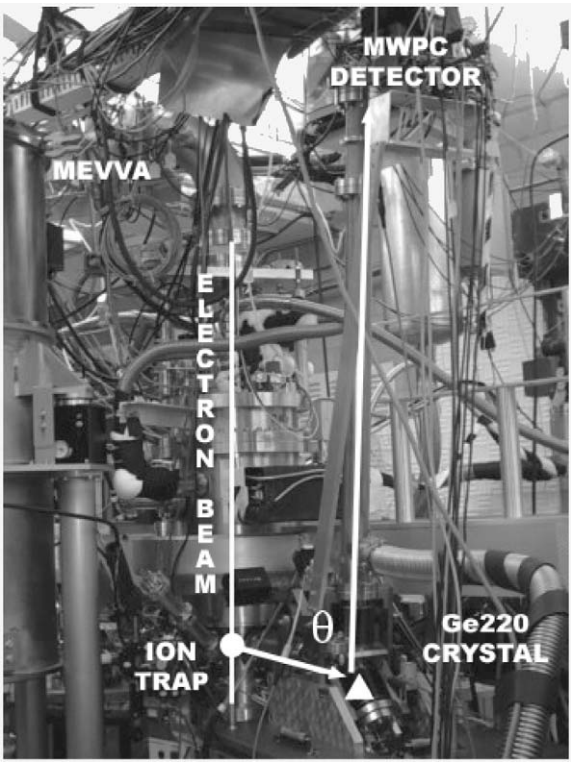

Fig. 3. EBIT and Johann spectrometer. Ion injection device, electron beam, trap region, X-ray beam path, diffracting crystal and detector system are also indicated. The angle of diffraction used for calibration is also indicated by θ.

3. Spectrometer

The main problems associated with the EBIT are the relatively low flux (of order 0.5 Hz count rate) and the possibility of beam drift which causes slight changes in the spatial position of the trapped ions and thus the photon source. A Johann-curved crystal spectrometer is used to offset these effects (Chantler et al., 1999). The Rowland geometry associated with this type of spectrometer means that the system is relatively insensitive to small changes in the source position, unlike flat crystal spectrometers, which are extremely sensitive to this broadening effect. The crystal focusing allows the maximisation of photon flux collected.

The system used is illustrated in Fig. 3. Photons from the ion source are Bragg diffracted and focused from a curved Ge220 crystal onto the detector. The angle of diffraction is recorded to high accuracy using a set of gravity referenced sensors known as inclinometers.

4. Systematics

An absolute energy calibration of the spectrometer is critical to the work. A dispersion function is constructed to relate energy of the diffracted photons to the diffraction angle ($E(\theta)$). A fluorescent source is used, the targets of which are five thin foils of type Sc, Ti, V, Cr, and Mn. By driving the spectrometer to the angles at which each of the characteristic spectral lines is observed and recording the diffraction angle, the dispersion function can be determined. The energy of the photons of interest can then be ascribed simply by measuring the angle of diffraction. The goal is to minimise the uncertainty associated with this function.

Systematic shifts caused by the dynamical diffraction of X-rays by the crystal itself are often over looked in much of the literature. When labelling a spectral line with a diffraction angle one must consider a modified Bragg law. Curved crystal diffraction modelling code (Chantler, 1992) allows us to quantify and reduce uncertainties of order 200 ppm in the dispersion function determination to around 5 ppm. It is not uncommon for published experimental results to contain no mention of uncertainties due to the spectrometer system used.

Monitoring, measurement and reduction of mechanical vibration of the spectrometer is vital. The spectrometer is mechanically robust and stable. A system of inclinometers and a thermocouple is also used so that continuous measurement of the system position and temperature such that compensation for any detector position drifts may be made. The detection system

Table 1
Error budget from the helium-like vanadium measurement as compared to the results achieved at the latest round of experiments

Error sources (ppm)	He-like V	He-like Ti (future?)
Inclinometry and related contributions		1–5?
New systematics included above		1–5?
Statistical contributions to dispersion function		3–5?
Total dispersion function determination	20	4–10?
Reference wavelengths	12	1–4?
Statistical uncertainty of the W-line	10	<10?
Diffraction theory	6	1–4?
Temperature and Doppler broadening	5	1–2?
Total for the W-line	27	?
Other resonance lines	$x = 40$, $y = 33$, $z = 28$	

Independent uncertainty contributions are summed in quadrature. Many of the systematic errors will be reduced with the final Ti^{20+} result predicted to have an uncertainty of between 15 and 20 ppm.

records the time of arrival of the photons (pseudo-event mode data collection), so that the correlation between detector position and photon position on the detector can be used to offset peak broadening due to vibrations. This has suppressed the uncertainty in results due to stability and temperature to 1–5 ppm.

The flux of the system has also been increased due to a larger effective detector area, faster software system for pseudo-event mode count collection and the ability to cleanly discriminate against cosmic rays or spurious counts in low-flux operation. This has halved the uncertainty due to count statistics and noise compared to previous work by this group (Kinnane et al., 2005).

We have no direct control over the uncertainty associated with assigning energies to the characteristic spectral lines in deriving the dispersion function. The metrological standards for characteristic K spectral lines are the tabulations of Bearden (1967) and Deslattes et al. (2003). Uncertainties associated with the tabulations are now a major limitation on results due to rapid development in the ability to quantify and suppress experimental uncertainties. The uncertainty of the assigned energy of vanadium Kβ spectral peak is approximately 14 ppm. Therefore, new experimental tabulations are required before uncertainties can be reduced to the sub-parts-per-million level.

However, we have developed an approach to the transfer of accuracy which involves an additional error component of only 1 ppm in linking lower-resolution spectra in a generalised geometry to the absolute standards, and we have redefined the method for using these earlier tables (Chantler et al., 2006). Assigning peak locations to the calibration spectra is relatively difficult due to the asymmetries in the peaks caused by solid state and satellite effects. This work has undertaken an extensive review of the fitting procedures used for the calibration spectra. This involves modelling the behaviour of the fit parameters associated with the fluorescence source spectral lines as a function of Z. Modelling reduces the transfer of peak energy uncertainties to less than 1 ppm contributions to the final result.

Past work by this group has produced results for the w-, x-, y- and z-transition energies in V^{21+} using these techniques which have resulted in the lowest quoted uncertainties in this region of Z to date (Chantler et al., 2000). Table 1 presents the error budget from that work as well as the results expected for the, yet to be completed, Ti^{20+} experiment. Many of the systematic errors will be reduced in comparison to the vanadium with the final result predicted to have an uncertainty of between 15 and 20 ppm.

The value in the right-hand column for dispersion function uncertainty is the level that can be achieved with relatively little effort if new X-ray standard tabulations are completed.

5. Future work

The field of bound state QED requires carefully conducted, highly accurate experimental results for testing. The work presented here involves measurement of the transition energies in highly charged medium-Z ions in which the bound state QED contributions are pronounced. The use of an EBIT for creating the required conditions has significant advantages. Extensive investigation of current limiting factors has led to significant reductions in the overall uncertainty as compared to previous work.

In the near future, further experiments will be undertaken to measure the Ti^{21+} transition energies. This will allow comparison with the helium-like results. This work will be extended to higher Z elements with

further major improvements made to all aspects of the experiment such that higher order bound state QED calculations may be tested and quantified.

Acknowledgements

The support and efforts in the experimental data collection and scheduling of the NIST EBIT group and in particular Larry Hudson, John Gillaspy, Albert Henins, Endre Takacs Joseph Tan and Joshua Pomeroy are gratefully acknowledged.

References

Bearden, J.A., 1967. X-ray wavelengths. Rev. Mod. Phys. 39, 78.

Chantler, C.T., 1992. X-ray-diffraction of bent crystals in Bragg geometry. 1. Perfect-crystal modeling. J. Appl. Crystallogr. 25, 674–693.

Chantler, C.T., Paterson, D., Hudson, L.T., Serpa, F.G., Gillaspy, J.D., Takacs, E., 1999. Precision X-ray spectroscopy at the NIST electron-beam ion trap: resolution of major systematic error. Phys. Scr. T80B, 440–442.

Chantler, C.T., Paterson, D., Hudson, L.T., Serpa, F.G., Gillaspy, J.D., Takacs, E., 2000. Absolute measurement of the resonance lines in heliumlike vanadium on an electron-beam ion trap. Phys. Rev. A 62, 042501/1-13.

Chantler, C.T., Kinnane, M.N., Su, C.H., et al., 2006. Characterization of K alpha spectral profiles for vanadium, component redetermination for scandium, titanium, chromium, and manganese, and development of satellite structure for $Z = 21$ to $Z = 25$. Phys. Rev. A 73 Art. No. 012508.

Chen, M.H., Cheng, K.T., Johnson, W.R., 1993. Relativistic configuration-interaction calculations of $N = 2$ triplet-states of helium-like ions. Phys. Rev. A 47, 3692–3703.

Deslattes, R.D., Beyer, H.F., Folkmann, F., 1984. Determination of the 1s Lamb shift in one-electron argon recoil ions. J. Phys. B 17, L689–L694.

Deslattes, R.D., Kessler, E.G., Indelicato, P., de Billy, L., Lindroth, E., Anton, J., 2003. X-ray transition energies: new approach to a comprehensive evaluation. Rev. Mod. Phys. 75, 35–99.

Drake, G.W., 1988. Theoretical energies for the $N = 1$-state and 2-state of the helium isoelectronic sequence up to $Z = 100$. Can. J. Phys. 66, 586–611.

Eides, M.I., Grotch, H., Shelyuto, V.A., 2001. Theory of light hydrogenlike atoms. Phys. Rep. 342, 63–261.

Indelicato, P., 1988. Multiconfiguration Dirac–Fock calculations of transition energies in 2 electron ions with 10-less-than-or-equal-to-Z-less-than-or-equal-to-92. NIM B 31, 14.

Karshenboim, S.G., 2004. Precision study of positronium: testing bound state QED theory. Int. J. Mod. Phys. A 19, 3879–3896.

Kinnane, M.N., Kimpton, J.A., de Jonge, M.D., et al., 2005. The correction of systematic image deformations inherent to two-dimensional proportional counters. Meas. Sci. Technol. 16 (11), 2280–2286.

Myers, E.G., Howie, D.J.H., Thompson, J.K., Silver, J.D., 1996. Hyperfine-induced 1s2s S-1(0)–1s2p P-3(0) transition and fine-structure measurement in heliumlike nitrogen. Phys. Rev. Lett. 76, 4899–4902.

Niering, M., Holzwarth, R., Reichert, J., Pokasov, P., Udem, T., Weitz, M., Hansch, T.W., Lemonde, P., Santarelli, G., Abgrall, M., Laurent, P., Salomon, C., Clairon, A., 2000. Measurement of the hydrogen 1S–2S transition frequency by phase coherent comparison with a microwave cesium fountain clock. Phys. Rev. Lett. 84, 5496–5499.

Plante, D.R., Johnson, W.R., Sapirstein, J., 1994. Relativistic all-order many-body calculations of the $N = 1$ and $N = 2$ states of helium-like ions. Phys. Rev. A 49, 3519–3530.

Silver, J.D., Varney, A.J., Margolis, H.S., et al., 1994. The Oxford electron-beam ion-trap—a device for spectroscopy of highly-charged ions. Rev. Sci. Instrum. 65, 1072–1074.